

Effect of head-group size of some tetradecylalkylammonium bromide surfactants on obtaining the lyotropic biaxial nematic phase

Erol Akpinar^{1,a}, Emre Guner¹, Oznur Demir-Ordu¹, and Antônio Martins Figueiredo Neto²

¹ Bolu Abant Izzet Baysal University, Faculty of Arts and Sciences, Department of Chemistry, 14030, Golkoy, Bolu, Turkey

² Instituto de Física, Universidade de São Paulo, Rua do Matão, 1371, São Paulo - SP, 05508-090, Brazil

Received 1 November 2018 and Received in final form 4 March 2019

Published online: 8 April 2019

© EDP Sciences / Società Italiana di Fisica / Springer-Verlag GmbH Germany, part of Springer Nature, 2019

Abstract. Lyotropic quaternary mixtures of some tetradecylalkylammonium bromide surfactants were prepared to examine the effect of the size of the surfactant head group on the stabilization of different lyotropic nematic phases. The lyotropic mixtures were prepared by the addition of the tetradecylalkylammonium bromides (TTAABr) in the mixture of NaBr/decanol (DeOH)/water. The uniaxial to biaxial nematic phase transitions were determined via laser conoscopy. Some micellization parameters such as critical micelle concentration, degree of counterion binding and micellization Gibbs energy were evaluated from the electrical conductivity measurements of diluted binary surfactants/water solutions. The results indicate that the head-group size of the surfactant molecules influences the amphiphilic molecular aggregate topology. Moreover, the effective area per surfactant head group is a key parameter on stabilizing the lyotropic biaxial nematic phase.

1 Introduction

Lyotropic nematic liquid crystals have been investigated for several years to clarify their stabilization mechanisms. Early studies about the orientation of the director of uniaxial nematic phases subjected to external magnetic fields showed that it depends on the shapes and symmetry of the micelles [1–4]. For instance, in uniaxial discotic nematic (N_D) and calamitic nematic (N_C) phases, local directors exhibit a preferred alignment in the perpendicular and parallel directions, respectively, with respect to the magnetic field. The biaxial nematic phase, N_B , was discovered in 1980 [5]. This phase was found to be (mainly) located between the two uniaxial phases in experimental phase diagrams. The uniaxial to biaxial nematic phase transitions were shown to be of second order [6–12], as predicted by a Landau-type mean-field theory [13,14]. From the symmetry point of view, this indicates the occurrence of continuous modifications of the dimensions of the same kind (symmetry) of micelles.

There are still in the literature controversies about the stabilization mechanism of the lyotropic biaxial nematic phase. Some authors claimed that the biaxial nematic phase would be a result of the coexistence of two

uniaxial phases [15]. On the other hand, other scientists asserted that the biaxial nematic phase is a distinct thermodynamically stable phase [8–11,16–18].

More recently, Akpinar and Neto [9–11,19,20] reported on how the choice of the surfactants, co-surfactants, electrolytes and relative concentrations of the mixture constituents play a significant role on the stabilization of the different nematic phases, in particular, the biaxial one. Depending on the lyotropic phase desired, co-surfactants and/or electrolyte may be added into the surfactant/water mixture. The effects of: a) the alkyl chain length of both surfactant and alcohol molecules [9,11], and b) the specific interactions between the ionic species, surfactant head groups and ions of electrolytes, at the micelle surfaces [19,20] on the stabilization of the nematic phases were investigated. For instance, while the strong and weak interactions between the surfactant head groups and electrolyte ions give rise to the formation of N_D and N_C phases, respectively, it is possible to obtain the N_B phase in the case of the intermediate level of those interactions at micelle's surface. Of course, these different interactions change the curvature of the micelle's surface causing different packing geometry of the surfactant molecules in the micelles.

Since the basic units of both lyotropic liquid crystals and isotropic (dilute) micellar solutions are micelles, they have some similar properties. One of the most

^a e-mail: akpinar_e@ibu.edu.tr

common properties is that if an electrolyte is added to the solutions, micelles grow in both solutions by changing the packing geometry of the surfactants [10, 21–24]. Many studies reported in the literature showed that the presence of the electrolytes in isotropic micellar solutions changes the micelle shapes from sphere to rod or lamellae or disk, in the case of direct micelle. This change is followed by the packing parameter of the surfactants in the isotropic micellar solutions. Dawin *et al.* [24] reported that the packing parameter also gives useful information about the stabilization of lyotropic phases. They evaluated the change in the packing parameter from isotropic to nematic phase (T_{NI}) to nematic to lamellar (T_{NL}) phase transitions. They observed that the packing parameter increases from T_{NI} to T_{NL} , as observed in isotropic micellar solutions. Consequently, the information obtained from isotropic micellar solutions may be applied to lyotropic nematic phases [10, 25].

The change of the micelle curvature by addition of electrolyte into the micellar solutions is well known. Indeed, the effect depends onto which extent the ionic species form ion pairs at the micelle's surface. In other words, the interactions at micelle's surface modify their shapes by changing the packing of the surfactants.

Now, the question is how can we modify the curvature of the micelle's surface at constant electrolyte concentration to obtain different lyotropic nematic phases, or other phases such as lamellar or hexagonal? An alternative way is the modification of the surfactant head groups. To do so, we synthesized some surfactant molecules, tetradecylalkylammonium bromides, providing the modification in the size of the surfactant head group. By this way, we change the strength of the interactions between the head groups and the ions (counterions of the surfactants and/or ions of electrolytes).

In this study, we aimed to see the effect of the head-group size of the surfactants to stabilize different lyotropic nematic phases. Thus, researchers may decide which surfactant should be more adequate to obtain the lyotropic biaxial nematic phase. The experimental design of this study is: in the first part, we examined the lyotropic liquid-crystalline properties of mixtures with tetradecylalkylammonium bromides by means of laser conoscopy and polarizing optical microscope; in the second part, we studied the isotropic micellar solutions of those surfactants by electrical conductivity; then, we combined all results to understand the role of the size of the surfactant head group on the stabilization of the different lyotropic nematic phases.

2 Experimental

All chemicals were purchased from Sigma, Merck and Aldrich in high purities (> 99%). Tetradecyltrimethylammonium bromide (TTMABr) was commercially available. Other tetradecylalkylammonium bromides, fig. 1 (tetradecyltrimethylammonium bromide, TDMABr; tetradecyltrimethylammonium bromide, TDMEABr; tetradecyltrimethylammonium bromide, TDEMABr; tetradecyltrimethylammonium bromide, TTEABr; tetradecyltrimethylammonium bromide, TTPABr; tetradecyltrimethylammonium bromide, TTBABr).

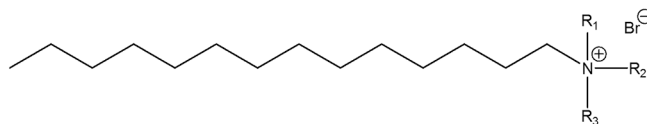


Fig. 1. Molecular structure of tetradecylalkylammonium bromides: TDMABr ($\text{R}_1=\text{H}$, $\text{R}_2=\text{R}_3=\text{CH}_3$), TTMABr ($\text{R}_1=\text{R}_2=\text{R}_3=\text{CH}_3$), TDMEABr ($\text{R}_1=\text{R}_2=\text{CH}_3$, $\text{R}_3=\text{CH}_2\text{CH}_3$), TDEMABr ($\text{R}_1=\text{CH}_3$, $\text{R}_2=\text{R}_3=\text{CH}_2\text{CH}_3$), TTEABr ($\text{R}_1=\text{R}_2=\text{R}_3=\text{CH}_2\text{CH}_3$), TTPABr ($\text{R}_1=\text{R}_2=\text{R}_3=\text{CH}_2\text{CH}_2\text{CH}_3$) and TTBABr ($\text{R}_1=\text{R}_2=\text{R}_3=\text{CH}_2\text{CH}_2\text{CH}_2\text{CH}_3$).

propylammonium bromide, TTPABr; tetradecyltributylammonium bromide, TTBABr) were synthesized with respect to their well-known synthesis procedure [26]. Ultrapure water was provided by Millipore Direct-Q3 UV, which furnishes water having $18.2 \text{ M}\Omega \cdot \text{cm}$ of resistivity at 25°C , for the preparation of isotropic micellar solutions and lyotropic liquid-crystalline mixtures.

Lyotropic liquid-crystalline mixtures were prepared by weighing the ingredients with a 5-digit balance (Radwag AS82/220.R2) into glass test tubes, which was then well closed with a cap and parafilm. The homogenization of the samples was provided by applying vortex (Velp TX4 with IR sensor) and centrifuging (Hettich EBA20) occasionally during some hours. Polarizing optical microscopy measurements were performed by Nikon Eclipse E200POL (Japan) microscope. A small portion of the sample was transferred into a rectangular microscope slides ($0.200 \text{ mm} \times 2.00 \text{ mm}$ - thickness \times width), followed by closing their ends with a specific photopolymer (Medental, USA) on which UV-light was applied to prevent water loss from the microscope slides. The microscope slides were placed in a precise temperature control unit (Linkam LTS120E with a temperature stability of, at least, 0.1°C). A water circulation system (Polyscience SD07R with an accuracy of $\pm 0.04^\circ\text{C}$) provided the homogenous heat distribution in the temperature-control unit.

The laboratory frame axes were chosen as follows: the horizontal plane consisted of two orthogonal axes 1 and 2, and axis 3 was vertical to the horizontal plane. While the laser beam propagation direction was along axis 3, the magnetic field was aligned along the axis 1. By this configuration, three different refractive indices are defined as n_1 , n_2 and n_3 . Two optical birefringences are measured: $\Delta n = n_2 - n_1$ and $\delta n = n_3 - n_2$. The anisotropic part of the optical susceptibility ($\bar{\varepsilon}_a$), written in terms of the birefringences, may be assumed as the second-rank tensor order parameter to describe the phase transitions in lyotropics [27]. The diagonal elements of this tensor ($\varepsilon_{a1}, \varepsilon_{a2}, \varepsilon_{a3}$), written in terms of the birefringences and the average index of refraction, $\langle n \rangle$:

$$\begin{aligned}\varepsilon_{a1} &= -\frac{4}{3}\langle n \rangle \left(\Delta n + \frac{\delta n}{2} \right); \\ \varepsilon_{a2} &= \frac{2}{3}\langle n \rangle (\Delta n - \delta n); \\ \varepsilon_{a3} &= \frac{4}{3}\langle n \rangle \left(\frac{\Delta n}{2} + \delta n \right),\end{aligned}$$

Table 1. Lyotropic mixture compositions in mole % and the observed phase types of the studied tetradecylalkylammonium bromides. The temperatures shown above the arrows are the phase transition temperatures.

TAABr	X _{TAABr}	X _{NaBr}	X _{DeOH}	X _{water}	Phase type
TDMABr	3.93	0.30	0.94	94.83	$L_\alpha \xrightarrow{44.6^\circ C} L_\alpha + I \xrightarrow{47.8^\circ C} I$
TTMABr	3.93	0.30	0.94	94.83	$N_C \xrightarrow{13.6^\circ C} N_B \xrightarrow{14.9^\circ C} N_D \xrightarrow{20.2^\circ C} I$
TDMEABr	3.93	0.30	0.94	94.83	$N_C \xrightarrow{12.7^\circ C} N_C + I \xrightarrow{18.4^\circ C} I$
TDEMABr	3.93	0.30	0.94	94.83	$N_C \xrightarrow{23.6^\circ C} N_C + H_1 \xrightarrow{54.2^\circ C} H_1 \xrightarrow{58.9^\circ C} H_1 + I \xrightarrow{64.8^\circ C} I$
TTEABr	3.93	0.30	0.94	94.83	$H_1 + I \xrightarrow{38.2^\circ C} I$
TTPABr	3.93	0.30	0.94	94.83	I
TTBABr	3.93	0.30	0.94	94.83	Phase separation

are used to calculate its symmetric invariants ($\sigma_1, \sigma_2, \sigma_3$):

$$\begin{aligned}\sigma_1 &= \varepsilon_{a1} + \varepsilon_{a2} + \varepsilon_{a3}; \\ \sigma_2 &= \frac{2}{3} (\varepsilon_{a1}^2 + \varepsilon_{a2}^2 + \varepsilon_{a3}^2); \\ \sigma_3 &= 4\varepsilon_{a1}\varepsilon_{a2}\varepsilon_{a3}.\end{aligned}$$

These invariants are employed to write down the free-energy expansion in the framework of the Landau mean-field theory. So, the optical birefringences, which are experimentally accessible, allows us to characterize the nematic phases as uniaxial or biaxial, besides precisely determine the phase-transitions temperature. Laser conoscopic was used to measure the temperature dependence of the birefringences of the three nematic phases. A small amount of water-based ferrofluid (Ferrotec) was added into the samples, as $1\mu\text{L}$ per 1g of the mixture, to obtain well-oriented nematic samples in a magnetic field ($\sim 2.3\text{kG}$, checked with Lakeshore 475 Model Gaussmeter). The samples were put between two 2.5cm of optical glasses (Helma) which were separated by 2.5mm of O-ring (Helma), *i.e.* 2.5mm thick samples were obtained. The temperature was controlled by a Lakeshore 335 model temperature controller (with Pt102 sensor and an accuracy of $\pm 0.001^\circ\text{C}$) and the heat distribution to all system was provided by a water circulating bath (Polyscience AD07R with an accuracy of $\pm 0.01^\circ\text{C}$). The good alignment of the sample, in particular in the biaxial phase, is essential to measure the optical birefringences. To achieve this condition, an external magnetic field (\vec{H}) of about 2kG is applied along a fixed direction. After some minutes we rotate, back and forth, the sample holder with respect to an axis perpendicular to the direction of \vec{H} of about $\pm 45^\circ$ until a good alignment is achieved. This is verified by inspecting (symmetry of the pattern and the contrast between clear and dark regions) the conoscopic fringe pattern. This process was shown to be very efficient to orient the N_B phase [28,29]. It was verified that this amount of ferrofluid doping does not change the phase transition temperatures and the phase topology [8,29].

Electrical conductivity measurements were performed in a Mettler Toledo S470 SevenExcellence setup at 30.0°C .

The dip-type conductivity cell was placed in a hand-made metallic (made from Al) sample holder in which water was circulated for providing stable temperature (circulating bath Polyscience SD07R). The conductivities were measured as a function of the surfactant concentration by the successive addition of stock solutions of tetradecylalkylammonium bromides into the cell containing ultrapure water. The stock solutions were added by $10\mu\text{L}$ of micropipette (Eppendorf). To keep the water loss at the minimum level, the conductivity cell was closed well, except during the addition of the stock solution. For each surfactant/water binary isotropic solutions, the conductivities were measured at ~ 50 different total surfactant concentrations until reaching the concentration of the surfactant to about 2–2.5 times of the critical micelle concentrations.

3 Results and discussions

Table 1 shows the compositions of the lyotropic mixtures of tetradecylalkylammonium bromide (TAABr) at constant constituents' concentrations by changing the surfactant head groups and the observed mesophases. By this way, we studied the effect of the size of the head groups on obtaining the biaxial nematic phases. As expected when the head-group size of TAABr molecules grows by the addition of $-\text{CH}_2$ group, the surface charge density of the head groups at the micelle's surface and the number of counterions bound to the micelle's surface decrease [26]. Because the counterions not only screen the repulsions at the micelle's surface but also affect the micelle surface curvature, the decrease in the counterion binding to the micelle's surface may cause the stabilization of different lyotropic liquid-crystalline structures. In this study, we observed the lyotropic lamellar (L_α), nematic (N), isotropic (I) and hexagonal (H_1) phases in the mixtures prepared (table 1). The textures of the lyotropic phases were inspected by polarizing optical microscopy, fig. 2.

In the lamellar phase, the surfactant molecules are packed in lamellae. In the case of the hexagonal phase, there exist long rod-like molecular aggregates, arranged in the hexagonal structure. If we compare both phases in

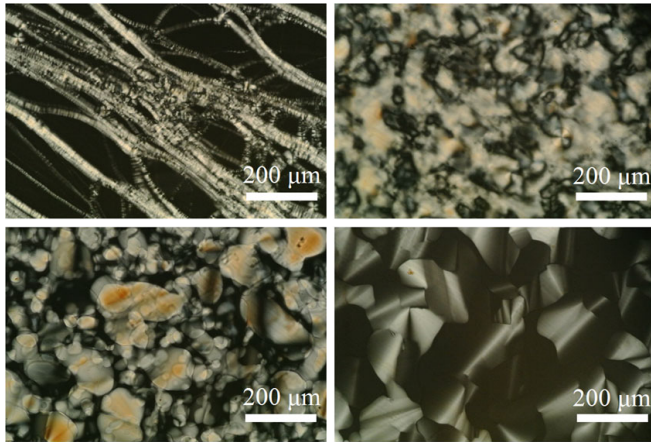


Fig. 2. Textures of the tetradecylalkylammonium bromide surfactants observed by polarizing optical microscopy: (a) L_α for TDMABr at 35.0°C , (b) N_c for TDEMABr at 15.0°C , (c) N_c+H_1 for TDEMABr at 25.0°C and (d) H_1 for TDEMABr at 55.0°C . Magnification of objective: $10\times$ and the sample thicknesses are $200\ \mu\text{m}$.

terms of the molecular-aggregates surface curvature, in the lamellar phase the aggregates have a lower surface curvature. This indicates that the repulsions between the surfactant head groups at the aggregates' surface are at the minimum level in the lamellar phase, and at the maximum level in the hexagonal phase. Then, the area per surfactant head group at the aggregates' surface in the lamellar phase is expected to be smaller than that in the hexagonal phase. Blackmore and Tiddy [30] reported the mesophase behavior of some dodecyl-, tetradecyl- and hexadecyltriaalkylammonium bromide surfactants in water, where their ionic head groups were trimethyl-, triethyl-, and tripropylammonium. They prepared and investigated the surfactants/water binary mixtures to compare the relative effect of the head-group size on the mesophase structures by “penetration optical microscope technique”. Their results are similar to those obtained in the present study, except that we prepared quaternary mixtures of surfactant/NaBr/DeOH/water. Moreover, they did not observe any nematic region in their phase diagrams.

The birefringences (Δn and δn , for details about the technique and definitions of these birefringences see [6, 8]) and the uniaxial to biaxial nematic phase transitions were determined by using the laser conoscopy. As discussed elsewhere [6], in the case of the uniaxial nematic phases, there is only one non-zero birefringence, and in the biaxial phase both birefringences are different from zero. The results are given in fig. 3. Previous experimental studies indicated that the higher the birefringences the bigger the micelles [11]. There exist three nematic phases in the mixture with TTMABr (fig. 3(a)). Additional $-\text{CH}_2$ in the head group of the surfactant molecules causes, first, the destabilization of both N_D and N_B phases (fig. 3(b)) and then, the appearance of the H_1 phase in the biphasic region (fig. 3(c)). The laser conoscopy results are in good agreement with the textures observed under the polarizing optical microscope (fig. 2(b), (c) and (d)). Specially, if

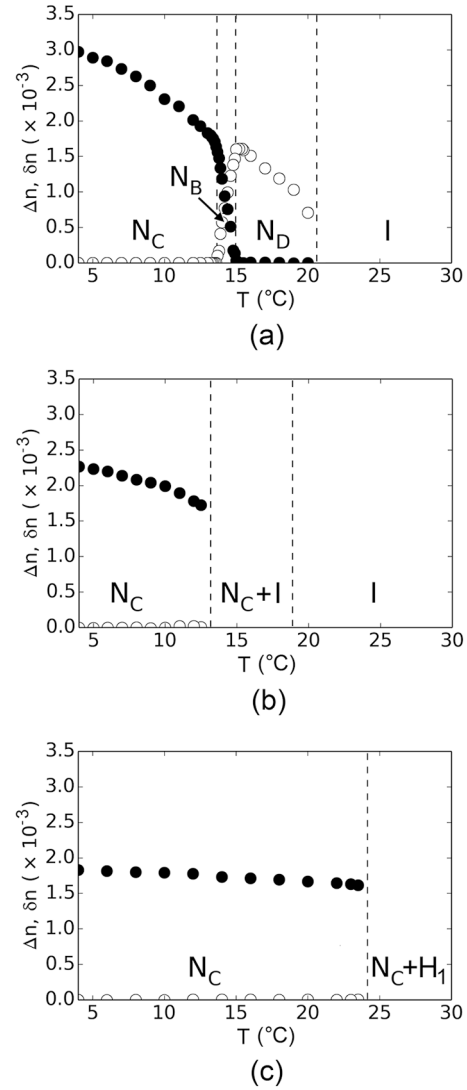


Fig. 3. Temperature dependence of the birefringences, Δn (●) and δn (○), for mixtures with (a) TTMABr, (b) TDMEABr, and (c) TDEMABr. N_D , N_B and N_c are the lyotropic discotic nematic, biaxial nematic and calamitic nematic phases, respectively. H_1 is the hexagonal phase. I represent the isotropic phase. For (a), the two-phase region $N_D + I$ between N_D and I phases was very narrow, less than 0.5°C .

we compare the birefringence values at 10.0°C , TTMABr, TDMEABr and TDEMABr have birefringences values of $\sim 2.3 \times 10^{-3}$, $\sim 2.0 \times 10^{-3}$ and $\sim 1.7 \times 10^{-3}$, respectively. This indicates that, as the head-group size increases, the micelle size gets smaller.

The authors of ref. [30] and refs. [31, 32] stated that there is a relation between the effective area per surfactant head groups (a_s) of TAABr bromide surfactants and the stabilization of different lyotropic structures. For instance, if a_s is bigger than $\sim 70\ \text{\AA}^2$, the hexagonal phase is most likely to be observed in the phase diagram. However, when the value of the a_s is smaller than $\sim 47\ \text{\AA}^2$, the hexagonal phase is not present in the phase diagram and just lamellar phase is stabilized. This is in good agree-

ment with our results given in table 1. From TDMABr to TTPABr, the surfactant head groups of TAABr molecules grow, *i.e.* their a_s values increase, and while the lamellar phase is not further observed, the nematic and hexagonal phases are stabilized.

In the present work, we focused our attention on the stabilization of the different lyotropic nematic phases and its relation with the parameter a_s . Before discussing its role, it is important to mention the mechanisms reported in the literature to explain the stabilization of the lyotropic nematic phases. In early studies, researchers assumed that the N_D and N_C phases consisted of disc-like (oblate ellipsoid) and cylindrical- or rod-like (prolate ellipsoid) micelles, respectively [15, 33–36]. They also proposed that the N_B phase is not a thermodynamically stable phase, being a coexistence of the two uniaxial N_D and N_C phases. However, some other researchers argued from theoretical and strong experimental evidences that the N_B phase is a thermodynamically stable distinct phase. Among the mechanisms stated in the literature, a model, so-called “Intrinsically Biaxial Micelles, IBM” model [28, 29, 37], seems us to be the best model to explain the stabilization of the lyotropic nematic phases. According to the IBM model, micelles present orthorhombic symmetry in the three nematic phases. A micelle could be sketched as a flat ellipsoid of mean axis A' , B' and C' , where C' corresponds to the micelle bilayer thickness. Temperature and relative concentrations of the mixture components lead to modifications in the dimensions A' and B' of them. When $A' \sim B'$, (static) orientational fluctuations that degenerate the axis perpendicular to the $A' \times B'$ are favored, and the N_D phase is stabilized. On the other hand, when $A' > B'$, (static) orientational fluctuations that degenerate the axis parallel to the A' dimension are favored, and the N_C phase is stabilized. The N_B phase is characterized by (static) orientational fluctuations of small amplitude. Different orientational fluctuations are the driving mechanisms for the stabilization of the three nematic phases. Furthermore, the continuous change in micelle sizes along two-dimensions (both A' and B') trigger the changes in the orientational fluctuations. Of course, the micelle-surface curvatures in the N_D phases are a little different than those in the N_C ones. This is supported by our results given in table 1. The TDMABr, which has the lowest a_s with respect to other studied surfactants, stabilizes the lamellar phase and, going from this surfactant to the TTEABr, the lamellar and N_D phases are destabilized, and the N_C , hexagonal and I phases appear. It means that the micelle’s surface curvatures in the N_D and N_C phases are not exactly same but similar to the lamellar and hexagonal ones, respectively, considering the a_s values given in the literature. The micelle’s surface curvature (related to a_s) is expected to increase in the sequence of L_α , N_D , N_B , N_C , H_1 and I. Dawin *et al.* [24] also reported the packing parameters (Π) of cesium perfluorooctanoate/D₂O lyotropic mixture as a function of the temperature, from nematic-isotropic to nematic-lamellar phase boundaries. According to their results, Π increases along the whole nematic phase region, towards the lamellar phase. Because Π is inversely proportional to a_s , $\Pi = V_{\text{hyd}}/(l_{\text{max}} a_s)$, where V_{hyd} and

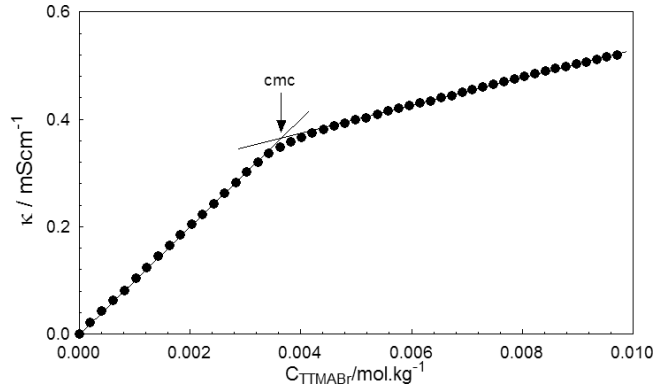


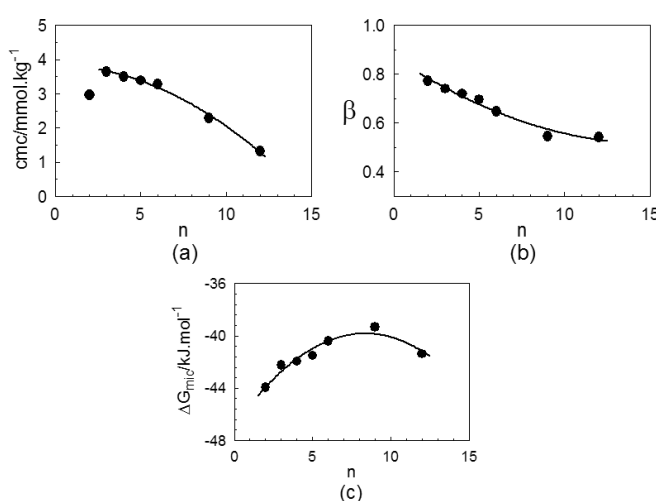
Fig. 4. Specific conductivity *versus* total TTMABr concentration at $30.0 \pm 0.1^\circ\text{C}$. For other TAABr surfactants, similar results were obtained. Solid lines are linear fits to the experimental points.

l_{max} are the volume of the hydrophobic chain and the maximum length of the hydrophobic chain of the surfactant, respectively, a_s decreases from the isotropic to the lamellar phase [24]. Thus, in our case, from the lamellar phase of TDMABr to the isotropic phase of TTEABr, passing through nematic and hexagonal phase region, V_{hyd} and l_{max} are constant for TAABr molecules. The different packing of the surfactant molecules, stabilizing different lyotropic structures, arises from change in the size of the head group (indeed, the change in a_s) of the TAABr molecules.

Our results indicate that the effective area per surfactant head group at the micelle’s surface is an important parameter to obtain different nematic phases, especially the N_B phase. However, it would be interesting to know how: a) the a_s values and b) the degree of counterion binding at the micelle’s surface change with the size of the head groups of the TAABr molecules. Some studies in the literature stated that, since lyotropic liquid crystals and the isotropic dilute micellar solutions consist of amphiphilic molecular aggregates, some parameters obtained from the latter one may be applicable to the former one [20, 24]. For instance, the addition of strong electrolytes to the mixtures gives rise to an increase in micelle dimensions in lyotropic mixtures and isotropic micellar solutions. Because of this, micellization parameters such as critical micelle concentrations (cmc) and the degree of counterion binding to the micelles, β , of tetradecylalkylammonium bromides, and micellization Gibbs energies as a function of the size of the head groups at 30.0°C were measured via electrical conductimetry technique. The cmcs of the surfactants correspond to a change of slope observed on the specific conductivity *versus* total surfactant concentration curve, fig. 4. Thus, two linear behaviors are obtained below and above the cmc, and the ratio of the slope of the latter curve to the former one gives the ionization degree of the counterion, α , which is related to β as $\alpha = 1 - \beta$. The micellization Gibbs free energies, $\Delta_{\text{mic}}G$, of the surfactants were evaluated by the equation, $\Delta_{\text{mic}}G = (1 + \beta)RT \ln X_{\text{cmc}}$, [38, 39], where R is the gas constant ($8.3145 \text{ J} \cdot \text{K}^{-1} \cdot \text{mol}^{-1}$), X_{cmc} is the mole frac-

Table 2. Critical micelle concentrations (cmc) of tetradecylalkylammonium bromide surfactants at 30.0 °C. The numbers between parentheses are from the literature.

Surfactant	cmc (mmol kg ⁻¹)	β	$\Delta_{\text{mic}}G$ (kJ · mol ⁻¹)	a_s (Å ²)
TDMABr	2.97 ± 0.04	0.772 ± 0.002	-43.94 ± 0.11	—
TTMABr	3.64 ± 0.05	0.740 ± 0.003	-42.24 ± 0.12	(87 ^h , 75.3 ^j)
	(3.61 ^a , 3.78 ^b , 3.84 ^c , 3.67 ^d)	(0.74 ^e , 0.73 ^f , 0.76 ^c , 0.77 ^a , 0.68 ^d)	(-42.5 ^c , -41.3 ^g , -40.62 ^d , -42.9 ^a)	
TDMEABr	3.50 ± 0.02	0.721 ± 0.002	-41.96 ± 0.08	—
TDEMABr	3.39 ± 0.02	0.697 ± 0.002	-41.51 ± 0.06	—
TTEABr	3.28 ± 0.01	0.647 ± 0.002 (0.65 ^e)	-40.40 ± 0.03	(90 ^g , 78.4 ^h)
TTPABr	2.29 ± 0.04	0.546 ± 0.004 (0.54 ^e)	-39.32 ± 0.10	(93 ^g , 81.4 ^h)
TTBABr	1.32 ± 0.01	0.542 ± 0.005 (0.54 ^e)	-41.37 ± 0.17	(97 ^g , 84.7 ^h)

^a From ref. [40].^b From ref. [41].^c From ref. [42].^d From ref. [43].^e From ref. [26].^f From ref. [44].^g From ref. [45].^h From ref. [46].^j From ref. [47].**Fig. 5.** (a) Critical micelle concentrations, (b) degree of counterion binding and (c) micellization Gibbs free energies of TAABr surfactants. n is the number of carbon atoms in the head groups of the surfactants, where $n = 2, 3, 4, 5, 6, 9$ and 12 correspond to TDMABr, TTMABr, TDMEABr, TDEMABr, TTEABr, TTPABr and TTBABr, respectively.

tion of the surfactant at the cmc in the absence of electrolyte (or salt), and T is the absolute temperature. The micellization Gibbs free energies are given in table 2. Our values of the cmc, β and $\Delta_{\text{mic}}G$ for tetradecyltrimethyl-

ammonium bromide at 30.0 °C are, within the experimental error, in good agreement with those from the literature [26, 40–47]. The change of cmc with an increase in the number of carbon atoms in the head groups, *i.e.* an increase in the size of the head groups, indicates that the cmc decreases slightly from TTMABr to TTEABr and strongly from TTEABr to TTBABr, fig. 5(a). In other words, the micellization becomes more favorable as the head groups of the surfactants grow. However, TDMABr, where two methyl and one hydrogen are bound to the central nitrogen atom in its head group, has lower cmc than TTMABr. In general, for ionic surfactants, the decrease in the cmc is the indicative of the increase in the β values or the decrease in the α values, which favors the micellization [42, 43, 45, 48]. But, in the case of tetradecylalkylammonium bromides, the decrease in their cmc values as a function of the head-group size, by the addition of $-\text{CH}_2$ group in their head groups, is a consequence of the increase in the hydrophobic character of the head groups. At the same time, while the dehydration of the head groups at the micelle surfaces occurs, the hydrophobic interactions between the neighboring head groups promote the micelle formation. Thus, less amount of counterions are bound to the micelle's surface, *i.e.* the degree of counterion binding decreases although their cmcs decrease, as the head group of the tetradecylalkylammonium bromides grow, fig. 5(b).

The behavior of the micellization Gibbs free energies with the number of carbon atoms in the head groups

of the surfactants, n , is in good agreement with the literature [26,48]. The value of the $\Delta_{\text{mic}}G$ of TTBABr is very similar to that of TDEMABr and this may be attributed to the penetration of some alkyl groups in the head group of the former one towards the deeper of the micelle's surface [26,49].

If the results of the isotropic micellar solutions of the tetradecylalkylammonium bromide surfactants are compared to the lyotropic liquid-crystal results, the a_s value of the surfactants seems to be a new control parameter to obtain different lyotropic phases, especially the N_B .

4 Conclusions

In this study, we investigated the effect of the size of the surfactant head groups on stabilizing the different nematic phases. To do so, we studied isotropic micellar solutions and lyotropic liquid-crystalline mixtures of tetradecylalkylammonium bromide surfactants. The laser conoscopy and polarizing optical microscopy results of the lyotropic nematic phases showed that the surfactant head-group size is one important parameter to obtain different lyotropic nematic phases. This parameter, the effective area per surfactant head group (a_s), has to be considered when choosing the suitable surfactant molecules to prepare a lyotropic mixture stabilizing the N_B phase.

The authors thank the Scientific and Technological Research Council of Turkey (TÜBİTAK) (grant number: 217Z079) from Turkey for financially supporting this work and CNPq (Conselho Nacional de Desenvolvimento Científico e Tecnológico) (465259/2014-6), FAPESP (Fundação de Amparo à Pesquisa do Estado de São Paulo) (2014/50983-3 and 2016/24531-3), CAPES (Coordenação de Aperfeiçoamento de Pessoal de Nível Superior), INCT-FCx (Instituto Nacional de Ciência e Tecnologia de Fluidos Complexos), and NAP-FCx (Núcleo de Apoio à Pesquisa de Fluidos Complexos) for financial support from Brasil.

Author contribution statement

EA and AMFN experimentally designed the study and interpreted the results. EG and ODO performed the experiments.

Publisher's Note The EPJ Publishers remain neutral with regard to jurisdictional claims in published maps and institutional affiliations.

References

1. K. Radley, L.W. Reeves, Can. J. Chem. **53**, 2998 (1975).
2. K. Radley, L.W. Reeves, J. Phys. Chem. **80**, 174 (1976).
3. B.J. Forrest, L.W. Reeves, C.J. Robinson, J. Phys. Chem. **85**, 3244 (1981).
4. J. Charvolin, A.M. Levelut, E.T. Samulski, J. Phys. (Paris) Lett. **40**, 587 (1979).
5. L.J. Yu, A. Saupe, Phys. Rev. Lett. **45**, 1000 (1980).
6. Y. Galerne, J.P. Marcerou, Phys. Rev. Lett. **51**, 2109 (1983).
7. E.A. Oliveira, L. Liebert, A.M.F. Neto, Liq. Cryst. **5**, 1669 (1989).
8. E. Akpinar, D. Reis, A.M.F. Neto, Eur. Phys. J. E **35**, 50 (2012).
9. E. Akpinar, D. Reis, A.M.F. Neto, Liq. Cryst. **39**, 881 (2012).
10. E. Akpinar, K. Otluoglu, M. Turkmen, C. Canioz, D. Reis, A.M.F. Neto, Liq. Cryst. **43**, 1693 (2016).
11. E. Akpinar, C. Canioz, M. Turkmen, D. Reis, A.M.F. Neto, Liq. Cryst. **45**, 219 (2018).
12. W.S. Braga, O.R. Santos, D.D. Luders, N.M. Kimura, A.R. Sampaio, M. Simões, A.J. Palangana, J. Mol. Liq. **213**, 186 (2016).
13. M.J. Freiser, Phys. Rev. Lett. **24**, 1041 (1970).
14. R. Alben, Phys. Rev. Lett. **30**, 778 (1973).
15. A. Stroobants, H.N.W. Lekkerkerker, J. Phys. Chem. **88**, 3669 (1984).
16. R. Bartolino, T. Chiaranza, M. Meuti, R. Compagnoni, Phys. Rev. A **26**, 1116 (1982).
17. C.C. Ho, R.J. Hoetz, M.S. El-Aasser, Langmuir **7**, 630 (1991).
18. A.M. Filho, A. Laverde, F.Y. Fujiwara, Langmuir **19**, 1127 (2003).
19. E. Akpinar, D. Reis, A.M.F. Neto, Liq. Cryst. **42**, 973 (2015).
20. E. Akpinar, M. Turkmen, C. Canioz, A.M.F. Neto, Eur. Phys. J. E **39**, 107 (2016).
21. J.N. Israelachvili, *Intermolecular and Surface Forces* (Academic Press, New York, 1991).
22. A. Sein, J. Engberts, Langmuir **11**, 455 (1995).
23. V.K. Aswal, P. Goyal, Phys. Rev. E **61**, 2947 (2000).
24. U.C. Dawin, J.P.F. Lagerwall, F. Giesselmann, J. Phys. Chem. B **113**, 11414 (2009).
25. E. Akpinar, S. Yurdakul, A.M.F. Neto, J. Mol. Liq. **259**, 239 (2018).
26. S.A. Buckingham, C.J. Garvey, G.G. Warr, J. Phys. Chem. **97**, 10236 (1993).
27. Y. Galerne, J.P. Marcerou, J. Phys. (Paris) **46**, 589 (1985).
28. A.M.F. Neto, Y. Galerne, A.M. Levelut, L. Liebert, J. Phys. (Paris) Lett. **46**, 409 (1985).
29. A.M.F. Neto, S.R.A. Salinas, *The Physics of Lyotropic Liquid Crystals: Phase Transitions and Structural Properties* (Oxford University Press, Oxford, 2005).
30. E.S. Blackmore, G.J.T. Tiddy, J. Chem. Soc. Faraday Trans. 2 **84**, 1115 (1988).
31. D.J. Mitchell, G.J.T. Tiddy, L. Waring, T. Bostock, M.P. McDonald, J. Chem. Soc. Faraday Trans. 1 **79**, 975 (1983).
32. G.J.T. Tiddy, in *Modern Trends of Colloid Science in Chemistry and Biology*, edited by H.F. Eicke (Birkhauser Verlag, Basel, 1985) p. 148.
33. Y. Rabin, W.E. McMullen, W.M. Gelbart, Mol. Cryst. Liq. Cryst. **89**, 67 (1982).
34. P.P. Muhoray, J.R. Bruyn, D.A. Dunmur, J. Chem. Phys. **82**, 5294 (1985).
35. R. Alben, J. Chem. Phys. **59**, 4299 (1973).
36. Z.Y. Chen, J.M. Deutch, J. Chem. Phys. **80**, 2151 (1984).
37. Y. Galerne, A.M.F. Neto, L. Liebert, J. Chem. Phys. **87**, 1851 (1987).

38. S.P. Moulik, M.E. Haque, P.K. Jana, A.K. Das, *J. Phys. Chem.* **100**, 701 (1996).
39. S.B. Velego, B.D. Fleming, S. Biggs, E.J. Wanless, R.D. Tilton, *Langmuir* **16**, 2548 (2000).
40. K. Maiti, D. Mitra, S. Guha, S.P. Moulik, *J. Mol. Liq.* **146**, 44 (2009).
41. P. Carpena, J. Aguiar, P. Bernaola-Galvan, C.C. Ruiz, *Langmuir* **18**, 6054 (2002).
42. C.C. Ruiz, L. Diaz-Lopez, J. Aguiar, *J. Colloid Interface Sci.* **305**, 293 (2007).
43. Md.M. Islam, M.R. Rahman, Md.N. Islam, *Int. J. Sci. Eng. Res.* **6**, 1508 (2015).
44. A.C.F. Ribeiro, V.M.M. Lobo, A.J.M. Valente, E.F.G. Azevedo, M.G. Miguel, H.D. Burrows, *Colloid Polym. Sci.* **283**, 277 (2004).
45. G.B. Ray, I. Chakraborty, S. Ghosh, S.P. Moulik, R. Palepu, *Langmuir* **21**, 10958 (2005).
46. P. Lianos, R. Zana, *J. Colloid Interface Sci.* **88**, 594 (1982).
47. R. Zana, *J. Colloid Interface Sci.* **78**, 330 (1980).
48. M.A. Rodriguez, M. Munoz, M.M. Graciani, M.S.D. Pachon, M.L. Moya, *Colloids Surf. A: Physicochem. Eng. Asp.* **298**, 177 (2007).
49. L. Maibaum, D. Dinner, D. Chandler, *J. Phys. Chem. B* **108**, 6778 (2004).